

1

2 **High Enrichment of Heavy Metals in Fine**

3 **Particulate Matter through Dust Aerosol Generation**

4

5 **Authors:** Qianqian Gao<sup>1,2#</sup>, Shengqiang Zhu<sup>1#</sup>, Kaili Zhou<sup>1,2</sup>, Jinghao Zhai<sup>3</sup>,  
6 Shaodong Chen<sup>1,2</sup>, Qihuang Wang<sup>1,2</sup>, Shurong Wang<sup>1</sup>, Jin Han<sup>1,2</sup>, Xiaohui Lu<sup>1,2</sup>,  
7 Hong Chen<sup>1</sup>, Liwu Zhang<sup>1,2</sup>, Lin Wang<sup>1,2</sup>, Zimeng Wang<sup>1,2</sup>, Xin Yang<sup>3</sup>, Qi Ying<sup>4</sup>,  
8 Hongliang Zhang<sup>\*1</sup>, Jianmin Chen<sup>1,2\*</sup> and Xiaofei Wang<sup>\*1,2</sup>

9

10 *<sup>1</sup>Shanghai Key Laboratory of Atmospheric Particle Pollution and Prevention,*  
11 *Department of Environmental Science and Engineering, Fudan University, Shanghai*  
12 *200433, China*

13 *<sup>2</sup>Shanghai Institute of Pollution Control and Ecological Security, Shanghai*  
14 *200092, China*

15 *<sup>3</sup>School of Environmental Science and Engineering, Southern University of*  
16 *Science and Technology, Shenzhen 518055, China*

17 *<sup>4</sup>Zachry Department of Civil Engineering, Texas A&M University, College*  
18 *Station, TX 77843, USA*

19

20 ***Atmospheric Chemistry and Physics***

21 **July 4<sup>th</sup>, 2023**

22 #These authors contributed equally to this paper

23 \*To whom correspondence should be addressed.

24 Correspondence to:

25 Xiaofei Wang: Email: [xiaofeiwang@fudan.edu.cn](mailto:xiaofeiwang@fudan.edu.cn) Tel: +86-021-31242526

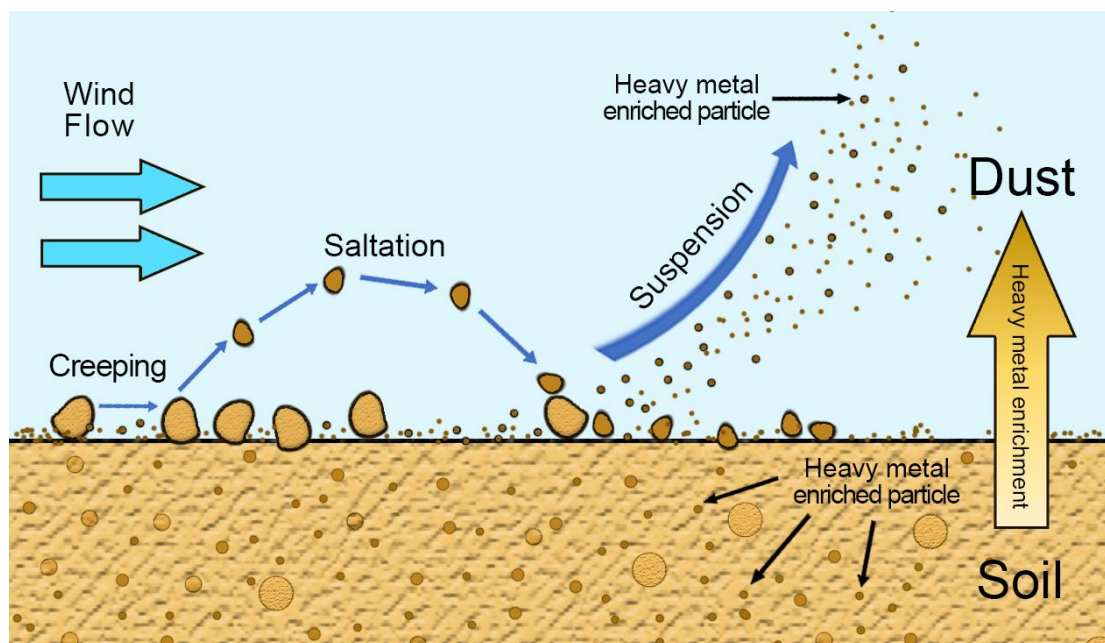
26 Jianmin Chen: Email: [jmchen@fudan.edu.cn](mailto:jmchen@fudan.edu.cn) Tel: +86-021-3124-2298

27 Hongliang Zhang: Email: [zhanghl@fudan.edu.cn](mailto:zhanghl@fudan.edu.cn) Tel: +86- 021-31248978

28 **Abstract**

29 Dust is a major source of atmospheric aerosols. Its chemical composition is often assumed to be  
30 similar to the parent soil. However, this assumption has not been rigorously verified. Here, we  
31 generated dust aerosols from soils to determine if there is particle size-dependent selectivity of  
32 heavy metals in the dust generation. Mn, Cd, Pb and other heavy metals were found to be highly  
33 enriched in fine ( $PM_{2.5}$ ) dust aerosols, which can be up to ~6.5-fold. To calculate the contributions  
34 of dust to atmospheric heavy metals, regional air quality models usually use the dust chemical  
35 profiles from the US EPA's SPECIATE database, which does not capture the correct size-dependent  
36 selectivity of heavy metals in dust aerosols. Our air quality modeling for China demonstrates that  
37 the calculated contribution of fine dust aerosols to atmospheric heavy metals, as well as their cancer  
38 risks, could have significant errors without using proper dust profiles.

39 **Graphical Abstract**



40

41

42 **Short Summary**

43 Dust is a major source of atmospheric aerosols. Its chemical composition is often assumed to be  
44 similar to the parent soil. However, this assumption has not been rigorously verified. Dust aerosols  
45 are mainly generated by wind erosion, which may have some chemical selectivity. Mn, Cd and Pb  
46 were found to be highly enriched in fine (PM<sub>2.5</sub>) dust aerosols. In addition, estimation of heavy  
47 metal emission from dust generation by air quality models may have errors without using proper  
48 dust profiles.

49

## 50 **1 Introduction**

51 The major sources of natural aerosols include mineral dust aerosols produced by wind erosion  
52 (Prospero et al., 2002). Dust aerosols are influenced by regional atmospheric circulation, soil  
53 characteristics and local weather conditions (Bryant, 2013; Ding et al., 2005; Huebert et al., 2003;  
54 Liu et al., 2004; Yang et al., 2008), mainly generated and aerosolized when strong wind passes over  
55 soil or sandy areas (Gillette and Goodwin, 1974). Recent studies show mineral dust aerosol accounts  
56 for approximately 40% of the mass fraction of natural atmospheric aerosol, with an estimated annual  
57 flux of  $\sim 2,000 \text{ Tg}\cdot\text{yr}^{-1}$  (Alfaro, 2008; Griggs and Noguera, 2002; Huneus et al., 2011; Textor et al.,  
58 2006). As the second-largest natural source of atmospheric aerosols in terms of mass flux, dust  
59 aerosol has a profound impact on the ecosystem (Middleton et al., 2019), especially the climate  
60 (Evan et al., 2014; Kok et al., 2018; Shao et al., 2013). Interactions between dust aerosols and water  
61 vapor play a critical role in cloud condensation and ice nucleation processes (Kaufman et al., 2002;  
62 Tang et al., 2016). Dust particles can be transported on large scales (Shao and Dong, 2006), and  
63 could act as a medium to transport toxic compounds, including heavy metals, which significantly  
64 harm human health, particularly the human respiratory system and even cause premature death  
65 (Urrutia-Pereira et al., 2021).

66 Atmospheric studies often assume that the chemical composition of aerosolized dust is similar to  
67 the parent soil (Gunawardana et al., 2012; Zhuang et al., 2001). The chemical composition of dust  
68 aerosol consists of a key part in source apportionment modeling (Balakrishna and Pervez, 2009;  
69 Samiksha et al., 2017; Santos et al., 2017; Ying et al., 2018). A critical approach in source  
70 apportionment modeling is the chemical transport model, which predicts the dust aerosol on global

71 and regional scales based on the prior knowledge of source emission, atmospheric transport, and  
72 chemical reaction process. SPECIATE is the EPA's speciation profiles repository of air pollution  
73 sources of volatile organic compounds (VOCs) and particulate matter (PM). Therefore, the US  
74 EPA's SPECIATE database is an important product to convert total emissions from specific sources  
75 into the speciated emissions needed for the chemical transport model. The previous study has  
76 combined the US EPA's SPECIATE database and air quality model to predict dust aerosols (Ying et  
77 al., 2018), based on the assumption of the chemical composition of dust aerosols is similar to the  
78 resuspended soil profiles.

79 Yet, dust generation and aerosolization are complex processes, which may have some chemical  
80 selectivity. Most small dust particles ( $< 20 \mu\text{m}$ ) are produced either by wind erosion, which leads to  
81 soil movements such as creeping, saltation, and suspension (Burezq, 2020) or sandblasting process,  
82 which leads soil particles ( $\sim 75 \mu\text{m}$ ) to be lifted by the wind, move in ballistic trajectories due to the  
83 combined effect of aerodynamic force and gravity force (Grini and Zender, 2004; Shao and Raupach,  
84 1993; Shao et al., 1996). The sandblasting efficiency of a soil particle is highly sensitive to its size  
85 (Grini and Zender, 2004; Grini et al., 2002). In addition, the chemical composition of soil particles  
86 can also vary with particle size. As smaller soil particles are more easily ejected, dust aerosol  
87 particles are unlikely to have exactly the same composition as their parent soils (Perlwitz et al., 2015;  
88 Wu et al., 2022). Dust deposited samples were the dust samples collected on the road or other  
89 surfaces using a brush and plastic tray (Shangguan et al., 2022), while dust aerosol samples were  
90 collected by filtering the air. Dust aerosols were produced by the ballistic impacts of wind-driven  
91 sand grains (Kok et al., 2023). Indeed, some previous studies do find that in the deposited dust  
92 samples (not dust aerosol samples), smaller particles tend to contain higher amounts of heavy metals

93 (Naderizadeh et al., 2016; Parajuli et al., 2016; Becagli et al., 2020). However, the heavy metal  
94 profiles for dust aerosols from the US EPA's SPECIATE database seem to have no such enrichment  
95 between each particle size, as Table S1 reports profile 41350 as an example. Although these profiles  
96 have been widely used in air quality modeling works (Lowenthal et al., 2010; Simon et al., 2010;  
97 Ashrafi et al., 2018), they were actually measured in the 1970s and 1980s with the resuspension of  
98 soil samples, which placed soil in a glass tube and drew air flow to blow and suspend the soil  
99 particles to the air (Miller et al., 1972). This method is not likely to produce realistic dust aerosols,  
100 as it does not simulate sandblasting process properly. It is not known whether using such a  
101 problematic dust profile could significantly impact air quality model calculations.

102

103 Here we examined the enrichment of heavy metals in the laboratory-generated dust aerosols. A dust  
104 aerosol generator that mimics realistic sandblasting and saltation was used to generate dust aerosol  
105 from a collection of soil samples (Lafon et al., 2014). The concentrations of heavy metals in soil  
106 and dust aerosols were measured by an inductively coupled plasma mass spectrometer (ICP-MS).  
107 In this study, some heavy metals, such as Mn, Cd, Zn and Pb, were found to be highly enriched in  
108 dust aerosols. Especially, the enrichment factors would be much higher for smaller dust aerosols. In  
109 addition, we also utilized a single particle aerosol mass spectrometer (SPAMS) to study heavy metal-  
110 containing dust aerosols before, during, and after a dust storm. Regional air quality models usually  
111 use problematic dust composition profiles from the US EPA's SPECIATE database. Herein we  
112 modeled the contribution of dust aerosol to atmospheric heavy metal loadings, utilizing a range of  
113 dust aerosol profiles determined in this laboratory study as well as the SPECIATE profile, to  
114 investigate whether using a proper dust profile is critical to air quality modeling and cancer risk

115 calculations.

## 116 **2 Materials and methods**

### 117 **2.1 Soil sample collection**

118 Fourteen samples were collected from the top 10 cm of the natural soil profile from various locations  
119 in dust source regions and Shanghai, China (Table S2, Fig. S1). S1-S4 were collected from dust  
120 sources on the northern slope of Yinshan Mountain in central inner Mongolia and the adjacent areas  
121 of the Hunshandake Sandy Land, S5-S12 were collected from dust sources of Hexi Corridor and  
122 Alxa Plateau, S13 was collected in Xinjiang Province, in the dust sources of the Taklimakan Desert,  
123 and S14 was sampled from Shanghai Yangpu District. Although the soil (S14) collected in Shanghai  
124 does not originate from a dust source region, it can still produce dust aerosols in some cases. For  
125 example, under dry weather conditions, the soil surface in the Shanghai area could serve as a  
126 significant local contributor to the generation of dust aerosols (Liu et al., 2016; Liu et al., 2020).  
127 During the prevailing dust storm periods from March to May, Shanghai is primarily influenced by  
128 dust originating from the western Inner Mongolia Gobi, deserts in the Tibetan Plateau, and arid  
129 deserts in northwest China (Fu et al., 2010; Fu et al., 2014; Sun et al., 2017). Soil texture  
130 determination was conducted according to the method outlined in a previous study (Kettler et al.,  
131 2001). Soil texture characterization was conducted based on the method outlined in a previous study  
132 (Kettler et al., 2001). Soil particle dispersion was achieved by adding hexametaphosphate (HMP)  
133 and sodium hydroxide (NaOH) to a soil sample (particle size < 2 mm) and shaking it for 16 hours.  
134 The percentage of sand and silt was obtained using a Laser Scattering Particle Size Distribution  
135 Analyzer (LA-960). Further details can be found in the SI. As shown in Table S2, they represent

136 several soil types: S1 was silty loam; S2, S4, S7, S10, S11 and S12 were sand; S3 was sandy loam;  
137 S5 and S6 were loam; S8 and S13 were loam sand; S9 and S14 were silty clay loam. Before dust  
138 aerosol generation, soil samples were placed in a fume hood and left to dry, without stirring or other  
139 treatment, before aerosolization. Fine and coarse dust aerosols (PM<sub>2.5</sub> and PM<sub>10</sub>) were produced  
140 with a GAMEL dust aerosol generator, which can realistically simulate the sandblasting process.  
141 Then, the pH of the soil was measured. Detailed information can be found in [Fig. S1](#) and [Table S2](#).

## 142 **2.2 Laboratory dust aerosol generation and collection**

143 A laboratory dust generator (GAMEL: “Générateur d’Aérosol Minéral En Laboratoire”) ([Lafon et](#)  
144 [al., 2014](#)) was used to produce dust aerosols from the soil samples. The GAMEL dust generator can  
145 realistically simulate the sandblasting process. Wind tunnels have the advantage of realistically  
146 simulating the generation of dust aerosols. However, conducting this study has certain drawbacks.  
147 These include the requirement for a substantial quantity of parent soils and the significant cost  
148 associated with eliminating ambient aerosol interference ([Alfaro et al., 1997](#); [Lafon et al., 2006](#);  
149 [Alfaro, 2008](#)). In GAMEL's dust production system, 10 g of each soil sample was added to a PTFE  
150 flask, which was agitated by a shaker simulating the sandblasting process to produce dust aerosols.  
151 A constant flow of particle-free air was passed through the dust-generating flask. The optimal  
152 generation parameter of the shaker was set at a frequency of 500 cycles/min according to [Lafon et](#)  
153 [al., 2014](#) with an airflow rate of 8 liter/min controlled by a Mass Flow Controller (MFC, Sevenstar,  
154 Beijing Sevenstar Flow Co., LTD). The sample stream was filtered through a cyclone and particles  
155 were collected on a 47 mm PVC film held in a metal frame filter holder (Pall Gelman, Port  
156 Washington, NY, USA). Dust-PM<sub>2.5</sub> and dust-PM<sub>10</sub> were obtained with or without an 8LPM cyclone,



157 respectively. The running time was 1 min. To obtain more dust aerosols in different size ranges, size-  
158 fractionated particle sampling of dust aerosols was carried out with 10-stage Micro-Orifice Uniform  
159 Deposit Impactor (MOUDI 110R; MSP) with size cut points of 10  $\mu\text{m}$ , 5.6  $\mu\text{m}$ , 3.2  $\mu\text{m}$ , 1.8  $\mu\text{m}$ , 1.0  
160  $\mu\text{m}$ , and 0.56  $\mu\text{m}$ . Analysis of the size distribution and chemical composition of dust generated by  
161 GAMEL and dust generated under natural conditions has shown that the GAMEL generator can  
162 produce realistic dust aerosol (Lafon et al., 2014). All the dust aerosol mass collected is shown in  
163 [Table S3](#) and [S4](#). The instrument setup is illustrated in [Fig. S2](#).

164

### 165 **2.3 Analysis of laboratory-generated dust aerosols**

166 The dust aerosol samples collected were weighed with an analytical balance and then put into 25 ml  
167 digestion tubes with 6 ml 69%  $\text{HNO}_3$  symmetrically. The temperature program of Microwave  
168 Digestion (Anton Paar) was as follows: initial temperature of 100  $^\circ\text{C}$  held for 5 min, then ramped  
169 to 140  $^\circ\text{C}$  for 5 min, and finally at 180  $^\circ\text{C}$  for 60 min. The whole process was holding 120 min.  
170 According to this study (Chang et al., 1984), almost all the heavy metal elements in the natural soil  
171 and dust aerosol in concentrated nitric acid were extracted using this experimental procedure. After  
172 digestion, the solution was acid-fed at 120  $^\circ\text{C}$  for 1.5 h, then deionized water (conductivity 18.25  
173  $\text{M}\Omega$ ) was added, the volume was constant with a 25 mL volumetric flask, and then passed through  
174 a 0.45  $\mu\text{m}$  membrane. The samples were diluted with 2%  $\text{HNO}_3$  by 4 times for further analysis.  
175 Three blank PVC film samples were digested using the same method for background control.

176

177 The heavy metal content was determined by inductively coupled plasma mass spectrometer (ICP-

178 MS; Agilent, 8900). Before analysis, tuning procedures including plasma parameter, ion  
179 transmission path, quadrupole mass spectrometer, and detector had been done. During analysis,  
180 standard solutions were prepared at concentrations of 0, 1, 2, 5, 10, 20, 50, and 100 µg/L. "In, Bi,  
181 and Rn" were used as internal standard elements, and were introduced into the nebulizer by mixing  
182 with the sample to be tested and the standard solution in the sampling pipeline by online addition,  
183 and the instrument drift and matrix effect were compensated. After each analysis of a sample, 2%  
184 dilute nitric acid was used to clean the injection line for 1 min, and then continue to collect the  
185 second sample to eliminate the memory effect of the previous sample.

186 A scanning electron microscope (SEM; Phenom Pro) equipped with an energy-dispersive X-ray  
187 detector was used for morphologies of particle examination at the voltage of 10 kV. All the samples  
188 (soil, PM<sub>2.5</sub> and PM<sub>10</sub>) were on the carbon conductive adhesive, then spray platinum to improve the  
189 conductivity. Here, the parent soil of S10 and generated PM<sub>2.5</sub> and PM<sub>10</sub> were examined.

190 Statistical analysis was performed using SPSS Statistics. The correlation analysis was conducted  
191 through Spearman's correlation and the significant difference was used with an independent sample  
192 T-test.

## 193 **2.4 Ambient dust aerosol measurements**

194 On May 23<sup>rd</sup>, 2018 (LT), on-site field measurements were conducted in Shanghai to assess the  
195 ambient dust particles. The measurements indicated an average wind speed of 2.2 m/s, which  
196 corresponds to a level of floating dust storm with a visibility of up to 10 km. The sampling was  
197 located on the sixth floor of the Environmental Science Building in Jiangwan Campus, Fudan  
198 University, a typical residential area in a heavily polluted urban area. The chemical composition of

199 individual ambient particles was measured by single particle aerosol mass spectrometry (SPAMS,  
200 Hexin Co., Ltd). Detailed information on SPAMS is available elsewhere (Li et al., 2011). An  
201 adaptive resonance theory-based clustering method (ART-2a) was used to classify the mass spectra  
202 generated and identify dust/heavy-metal-containing particles (Sullivan et al., 2007). The Hybrid  
203 Single-Particle Lagrangian Integrated Trajectory HYSPLIT-4 model developed by the ARL (Air  
204 Resources Laboratory) of the NOAA (National Oceanic and Atmospheric Administration), USA,  
205 was employed to compute hourly resolved 48 h air mass backward trajectories at 500 m arrival  
206 height (Lv et al., 2021; Pongkiatkul and Kim Oanh, 2007).

207

## 208 **2.5 Air quality model configuration and application**

209 The source-oriented Community Multiscale Air Quality (CMAQ) model v5.0.1 with an expanded  
210 Stratospheric and Air Pollution Research-99 (SAPRC-99) photochemical mechanism was applied  
211 to simulate PM<sub>2.5</sub> levels and track the sources of primary PM<sub>2.5</sub> (PPM<sub>2.5</sub>) in China during the entire  
212 year of 2013 (Guenther et al., 2012; Ying et al., 2018). The simulation domain covered China and  
213 its surrounding countries, with a horizontal resolution of 36 × 36 km<sup>2</sup> (127 × 197 grids).  
214 Anthropogenic emissions were based on the Multi-resolution Emission Inventory for China (MEIC,  
215 v1.3, 0.25° × 0.25°, <http://www.meicmodel.org>). Biogenic emissions were generated by the Model  
216 of Emissions of Gases and Aerosols from Nature (MEGAN) v2.1 (Guenther et al., 2012). The  
217 meteorological inputs for the CMAQ model were calculated by the Weather Research and  
218 Forecasting (WRF) model (<https://www2.mmm.ucar.edu/wrf/users>).

219

220 Five major source contributions (windblown dust, residential, transportation, power generation and  
221 industrial sources) to PM<sub>2.5</sub> were investigated based on the inventory-observation-constrained  
222 emission factors (Ying et al., 2018). Three control trials were conducted for each heavy metal  
223 according to measured soil, dust-PM<sub>2.5</sub> and the SPECIATE datasets from the four regions (three dust  
224 sources and Shanghai). It is worth noting that the emission factors for areas outside these four  
225 regions were estimated using Inverse Distance Weight (IDW) spatial interpolation methods. These  
226 methods were based on the dataset of emission factors within these four regions, which represent  
227 the amount of heavy metal emitted per kilogram of dust (Zhang and Tripathi, 2018). Each heavy  
228 metal source concentration from dust aerosol and all four sources were used to quantify the  
229 contribution on heavy metal concentrations in the atmospheric dust aerosols, which can be  
230 represented in Equation 1:

$$231 \quad R = \frac{E_i \times s_i \times a}{\sum_{i=1}^5 E_i \times s_i} \quad \text{Equation 1}$$

232 Where  $E_i$  is the PPM<sub>2.5</sub> emission from  $i^{th}$  source,  $s_i$  is the emission factor of the specific heavy metal  
233 from  $i^{th}$  source,  $a$  is the concentration of heavy metal in measured soil, dust-PM<sub>2.5</sub>, and the  
234 SPECIATE datasets.  $E_i$ ,  $s_i$ , and  $a$  are the values for dust.

235 In addition, the human health risk of heavy metals was assessed. Three main routes of chemical  
236 daily intake (CDI, mg kg<sup>-1</sup> day<sup>-1</sup>) of air heavy metals were: (1) direct ingestion of particles or gases  
237 existed in the air (CDI<sub>ing</sub>); (2) inhalation of suspended particles through mouth and nose (CDI<sub>inh</sub>);  
238 and (3) daily absorption of heavy metals through skin (CDI<sub>dermal</sub>) (Luo et al., 2012). To assess the  
239 carcinogenic and non-carcinogenic effects of heavy metals, we evaluated these effects in 13 age  
240 groups ranging from birth to ≤80 years old. These age groups are as follows: <1, 1 to <2, 2 to <3, 3  
241 to <6, 6 to <11, 11 to <16, 16 to <20, 21 to <31, 31 to <51, 51 to <61, 61 to <71, 71 to <81, and ≥81

242 years (Gholizadeh et al., 2019b). The variables and values used for estimating human exposure to  
 243 heavy metals were obtained from the U.S. Environmental Protection Agency (USEPA) and the U.S.  
 244 Department of Energy (USDoE) (Moya et al., 2011; Doe, 2011).  $CDI_{ing}$ ,  $CDI_{inh}$ , and  $CDI_{dermal}$   
 245 were calculated as:

$$247 \quad CDI_{ing} = C \times \frac{IR_{ing} \times EF \times ED}{BW \times AT} \times 10^{-6} \quad \text{Equation 2}$$

$$248 \quad CDI_{dermal} = C \times \frac{SA \times AF \times ABS_d \times EF \times ED}{BW \times AT} \times 10^{-6} \quad \text{Equation 3}$$

$$249 \quad CDI_{inh} = C \times \frac{IR_{inh} \times ET \times EF \times ED}{BW \times AT} \times 10^{-6} \quad \text{Equation 4}$$

250 Moreover, the total carcinogenic risk  
 251 (TCR) for each heavy metal were calculated by:

$$252 \quad \text{carcinogenic risk} = CDI_{ing,dermal,inh} \times CSF \quad \text{Equation 5}$$

$$253 \quad TCR = \sum risk = CDI_{ing} \times CSF_{ing} + CDI_{inh} \times IUR +$$

$$254 \quad CDI_{dermal} \times CSF_{ing}/ABS_{GI} \quad \text{Equation 6}$$

255  
 256 Here the  $IR_{ing}$  was Ingestion rate ( $\text{mg day}^{-1}$ ),  $EF$  was exposure frequency ( $\text{day year}^{-1}$ ),  $ED$  was  
 257 exposure duration (year),  $BW$  was body weight (kg),  $AT$  was Averaging time (day),  $SA$  was total  
 258 body skin surface area ( $\text{m}^2$ ),  $AF$  was skin adherence factor ( $\text{mg cm}^{-2}$ ),  $ET$  was exposure time (hour  
 259  $\text{day}^{-1}$ ),  $ABS_d$  was dermal absorption factor,  $IR_{inh}$  inhalation rate ( $\text{m}^3 \text{day}^{-1}$ ),  $ABS_{GI}$  was  
 260 gastrointestinal absorption factor,  $CSF$  was cancer slope factor. The values of these parameters could  
 261 be found in the previous study (Gholizadeh et al., 2019a).

262

## 263 **3 Results and discussion**

### 264 **3.1 Enrichment of heavy metals in fine dust aerosols**

265

266 [Fig. S3-S4](#) show the absolute concentrations of heavy metals in dust aerosols and their parent soils.

267 The concentrations of heavy metals in dust-PM<sub>10</sub> were similar to soil concentrations, which showed  
268 a significant correlation between soils and PM<sub>10</sub> (p<0.01) ([Fig. S5](#)). While the concentrations of  
269 heavy metals in dust-PM<sub>2.5</sub> were higher than those in soils, especially Mn, Ni, Cu and Zn, showed  
270 significant differences (p<0.001) ([Fig. S6](#)). This trend was consistent across all soil samples. The  
271 enrichment factor (EF) of heavy metals in dust aerosols relative to the parent soils was calculated  
272 with Equation 8.

$$273 \quad EF = \frac{C_1/m_1}{C_0/m_0} \quad \text{Equation 8}$$

274 Where C<sub>1</sub> is the heavy metal concentration in dust-PM; m<sub>1</sub> is the mass of dust-PM collected on the  
275 filter; m<sub>0</sub> is the mass of soil in the ICP-MS sample, and C<sub>0</sub> is the heavy metal concentration of the  
276 soil.

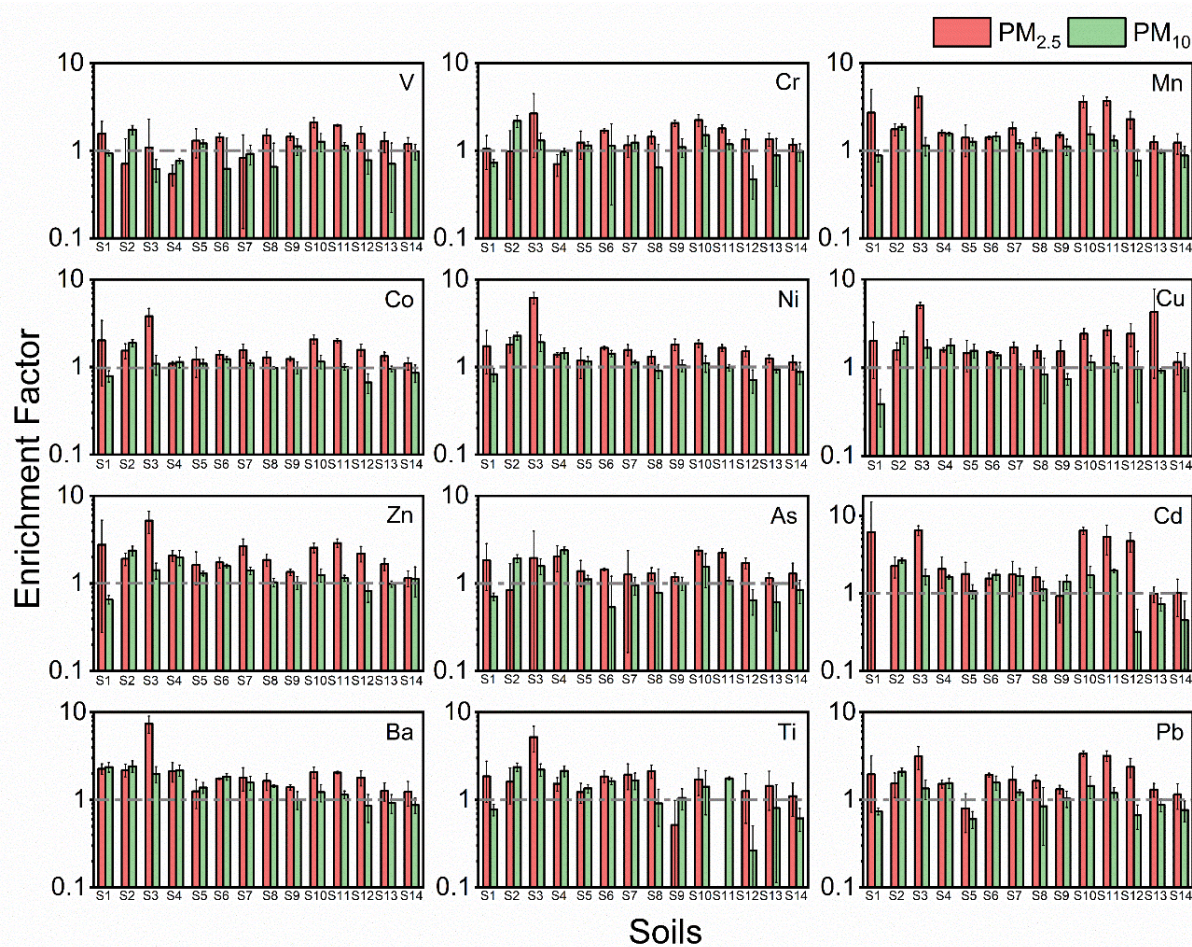
277

278 [Figures 1](#) and [S7](#) show that many heavy metals were highly enriched in fine dust aerosols (PM<sub>2.5</sub>),  
279 i.e., their absolute concentrations were significantly higher in fine dust particles than in the parent  
280 soil ([Fig. S6](#)). V, Cr, Mn, Co, Ni, Cu, Zn, As, Cd, Ba, Ti, and Pb were all enriched in dust-PM<sub>2.5</sub>  
281 during the process of dust formation. The following trend of heavy metal enrichment was  
282 established for dust-PM<sub>2.5</sub>: Cd > Zn > Ba > Cu > Mn > Pb > Ni > Ti > Co > As > Cr > V. Notably,  
283 the EFs of Cd were greater than 5 for soil S1, S10 and S11. No other literature has reported the  
284 enrichment of Cd or other heavy metals in dust aerosols. However, there is one study showing the

285 enrichment of water-soluble ions during dust aerosol production from soil (Wu et al., 2022). It  
286 reports that the EFs of  $\text{Ca}^{2+}$  ranged from approximately 5.6 to 223.1, and the EF values of  $\text{Mg}^{2+}$   
287 were between approximately 2.1 and 90.3 for dust- $\text{PM}_{2.5}$  from Sandy soils in the Taklamakan Desert.  
288 In this study, it is found that the EF of Cd and other metals falls within the range of EF for these  
289 water-soluble ions, consistent with the value reported by Wu et al., (2022). Fig. 1 also illustrates  
290 that all heavy metals were more highly enriched in smaller  $\text{PM}_{2.5}$  dust particles compared to larger  
291  $\text{PM}_{10}$  dust particles. For example, the Cd's EF reached ~6.4 and ~1.7 for dust- $\text{PM}_{2.5}$  and dust  $\text{PM}_{10}$ ,  
292 respectively, from soil S1. Most dust- $\text{PM}_{2.5}$  should originate from the small colloids in soil, which  
293 are defined as soil particles with less than 2  $\mu\text{m}$  in diameter. These soil colloids usually carry large  
294 amounts of negative charges, which can help adsorb many cations in soil, including various heavy  
295 metal ions (Brady and Weil, 2008). Thus, heavy metals are enriched in small soil aggregates. During  
296 the sandblasting process, the smaller soil grains, with higher heavy metal concentrations, are more  
297 likely to be ejected and form dust aerosols. The particle size dependence of heavy metal enrichment  
298 could have significant ramifications for the health impacts of dust aerosols. The dust aerosol size  
299 distribution of dust (Fig. S8) was also measured by an Aerodynamic Particle Sizer (APS,  
300 APS Model 3321; TSI Inc.; USA). It is found that the peak of the particle size distribution of dust  
301 aerosol was approximately at 2~3  $\mu\text{m}$ . Similarly, the scanning electron microscope (SEM) images  
302 of these dust aerosols (generated by S10) also show the presence of a large number of particles with  
303 sizes of 2~3  $\mu\text{m}$ . As particle size decreased, the shape of particles changed from flakes to rods,  
304 which means a larger surface area (Fig. S9). When examining the impact of soil texture on dust  
305 aerosol enrichment, first, notable variations were observed in the EF values from one soil texture,  
306 such as sandy soils, specifically S2, S4, S7, S10, S11, and S12. To assess the significance of these

307 variations, a one-way Analysis of Variance (ANOVA) was conducted using SPSS. In ANOVA, the  
308 *p-value* represents the probability of obtaining the observed differences in means (or more extreme  
309 differences) by random chance alone, assuming no true difference between the groups. A *p-value*  
310 below a predetermined significance level (commonly 0.05) indicates significant differences between  
311 the means of the compared groups. Specifically, for sandy soil, analysis results reveal significant  
312 variations between these six soils in terms of the EF values for both dust-PM<sub>2.5</sub> (*p-value*=0.004<0.05)  
313 and dust-PM<sub>10</sub> (*p-value*=0<0.05) (Table S5 and S6). These results indicate that there are significant  
314 differences in the EFs of heavy metals within the sandy soil group. Then, the variation between soil  
315 types was analyzed. For the six different types of soil samples, the results of ANOVA showed  
316 significant differences in the EFs of dust-PM<sub>2.5</sub> (*p-value*=0<0.05) and dust-PM<sub>10</sub> (*p-value* =0<0.05)  
317 among these soil types (Table S7 and S8). The differences among the six soils from different soil  
318 types were greater than those observed among the different soils in the same soil type, indicating a  
319 potential role of soil type in affecting EFs, which would require further study to elucidate. Detailed  
320 information was found in SI of Texture S3 and Table S5-S10.





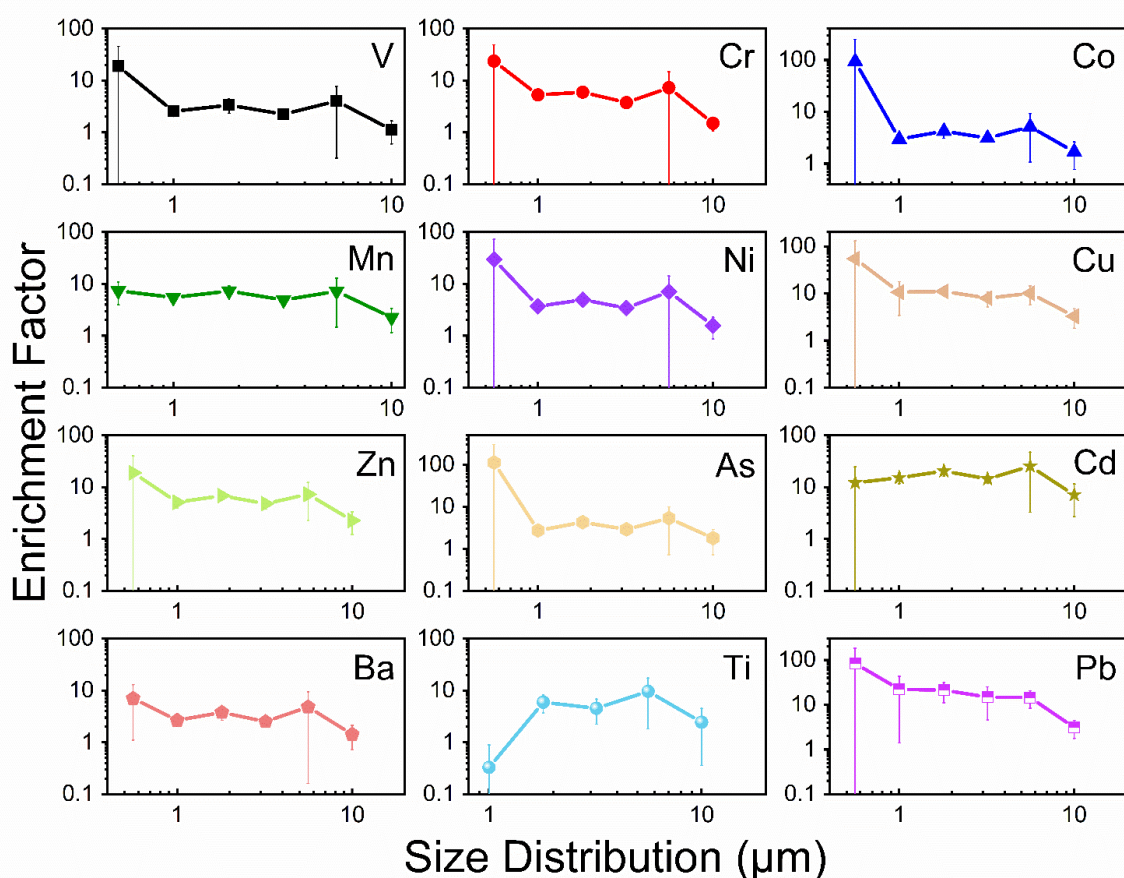
321

322 **Figure 1.** Enrichment Factors of PM<sub>2.5</sub> and PM<sub>10</sub>. Enrichment factors of heavy metals in dust  
 323 aerosols from soil S1-S14; red represents PM<sub>2.5</sub> and green represents PM<sub>10</sub>. The grey dotted line  
 324 represents the EF as 1. The whiskers on the bars represent the standard deviations of triplicates.

325

326 To investigate the link between dust particle size and heavy metal EFs in greater detail, a MOUDI  
 327 impactor was used to collect dust-PM from 0.56 to 10  $\mu\text{m}$  (absolute concentration obtained in [Fig.](#)  
 328 [S10](#)). Consistent with the results discussed above, the EFs for some heavy metals, such as Pb,  
 329 significantly increased with decreasing particle diameter ( $r = -1$ ,  $p < 0.01$ ) ([Fig. 2](#)). For the smallest  
 330 dust particles (0.56~1.0  $\mu\text{m}$ ), the EFs for Pb was approximately 83, an order of magnitude greater  
 331 than the EFs (~3) for the largest dust particles (>10  $\mu\text{m}$ ). V, Cr, Co, Mn, Ni, Cu, Zn, As, and Ba  
 332 show consistent trends, with EFs increasing as the particle size decreases. In detail, V (ranging from

333 ~1.1 to ~18.9), Cr (ranging from ~1.5 to ~23.7), Co (ranging from ~1.7 to ~93.7), Mn (ranging from  
 334 ~2.3 to ~7.4), Ni (ranging from ~1.6 to ~29.7), Cu (ranging from ~3.3 to ~54.3), Zn (ranging from  
 335 ~2.3 to ~19.0), As (ranging from ~1.8 to ~112.3), and Ba (ranging from ~1.4 to ~7.0), as the particle  
 336 size decreases from 10  $\mu\text{m}$  to 0.56  $\mu\text{m}$ . This results demonstrate that some heavy metals are indeed  
 337 enriched in smaller soil particles, which could be aerosolized during the sandblasting process. The  
 338 particle size dependence of heavy metal enrichment could have significant ramifications for the  
 339 health impacts of dust aerosols. In contrast, Cd's EFs remain relatively unchanged with varying  
 340 particle sizes. On the other hand, Ti exhibits an opposite trend, with EF values decreasing as the  
 341 particle size decreasing, and the reason for this difference requires further study.



342  
 343 **Figure 2.** Enrichment factors of heavy metals in dust aerosols with different particle size ranges.  
 344 The EF data were produced from the Soil S10, with diameters at above 10  $\mu\text{m}$ , 5.6-10  $\mu\text{m}$ , 3.2-5.6  
 345  $\mu\text{m}$ , 1.8-3.2  $\mu\text{m}$ , 1.0-1.8  $\mu\text{m}$  and 0.56-1.0  $\mu\text{m}$ . The whiskers on the bars represent the standard

346 deviations of triplicates.

347

### 348 **3.2 Modeling of the contributions of dust aerosols to atmospheric heavy metals** 349 **using the dust profiles from this study and the SPECIATE datasets**

350 It is necessary to know the sources of atmospheric heavy metals to effectively control their emission.

351 Air quality models with emission inventories can estimate the contributions of various sources to

352 atmospheric heavy metals. However, when estimating heavy metal emissions from dust production,

353 some widely used air quality models, such as the CMAQ model, typically use dust profiles from the

354 US EPA's SPECIATE datasets. As discussed in the introduction, this dust profile may be outdated

355 and cannot reflect realistic dust compositions. We used the CMAQ model to assess the potential

356 impact of dust aerosol profile in atmospheric dust aerosol using our measured profile and the profile

357 (No. 41350) from the SPECIATE datasets. The model tracked heavy metals in PM<sub>2.5</sub> in China for

358 the year 2013 (see Methods) from five major sources: windblown dust, residential, transportation,

359 power generation, and industry.

360

361 [Figure 3](#) shows the modeled contributions of the dust source to the Cr and Pb concentrations in

362 PM<sub>2.5</sub> for China, using the measured soil, dust-PM<sub>2.5</sub> profiles from this study, as well as the

363 SPECIATE composition profiles (see Methods). In addition, the modeled results for other metals,

364 such as As, Cu, Mn, Ti, and Zn were presented in [Fig. S11-15](#).

365

366 For atmospheric Cr, it is clear that the scenario of applying SPECIATE database significantly

367 underestimates the contribution of dust aerosol, with the highest value of  $\sim 0.08 \mu\text{g}/\text{m}^3$ , when

368 compared to the scenario of applying the measured dust-PM<sub>2.5</sub> profiles, which had the highest value  
369 of  $\sim 0.14 \mu\text{g}/\text{m}^3$ . For Pb, as shown in the right column of Fig. 3, the scenario of applying  
370 SPECIATE profile overestimates the contribution of dust aerosol, with the value up to  $\sim 0.4 \mu\text{g}/\text{m}^3$ ,  
371 when compared to the scenario of applying the measured dust-PM<sub>2.5</sub> profiles, which had the highest  
372 value of  $\sim 0.14$ . Uncertainties associated with the use of SPECIATE have also been identified in  
373 previous studies (Ho et al., 2003; Xia et al., 2017). Specifically, the dust PM<sub>2.5</sub> source profiles  
374 obtained from local studies indicated that SPECIATE overestimated the contributions of  
375 atmospheric K and Al by approximately 23%, while underestimating the contributions of Ca and  
376 Na by 50%. Additionally, the model represents the annual average data for the year 2013. Although  
377 there are some field studies conducted in the same year (Wang et al., 2021; Shi et al., 2018), there  
378 is no available annual average data for a direct comparison with the model results. These results  
379 demonstrate that the modeled heavy metal distribution in the atmosphere is quite sensitive to the  
380 input of dust composition profile, strongly suggesting that using a proper dust composition profile  
381 is a key in such air quality modeling.

382

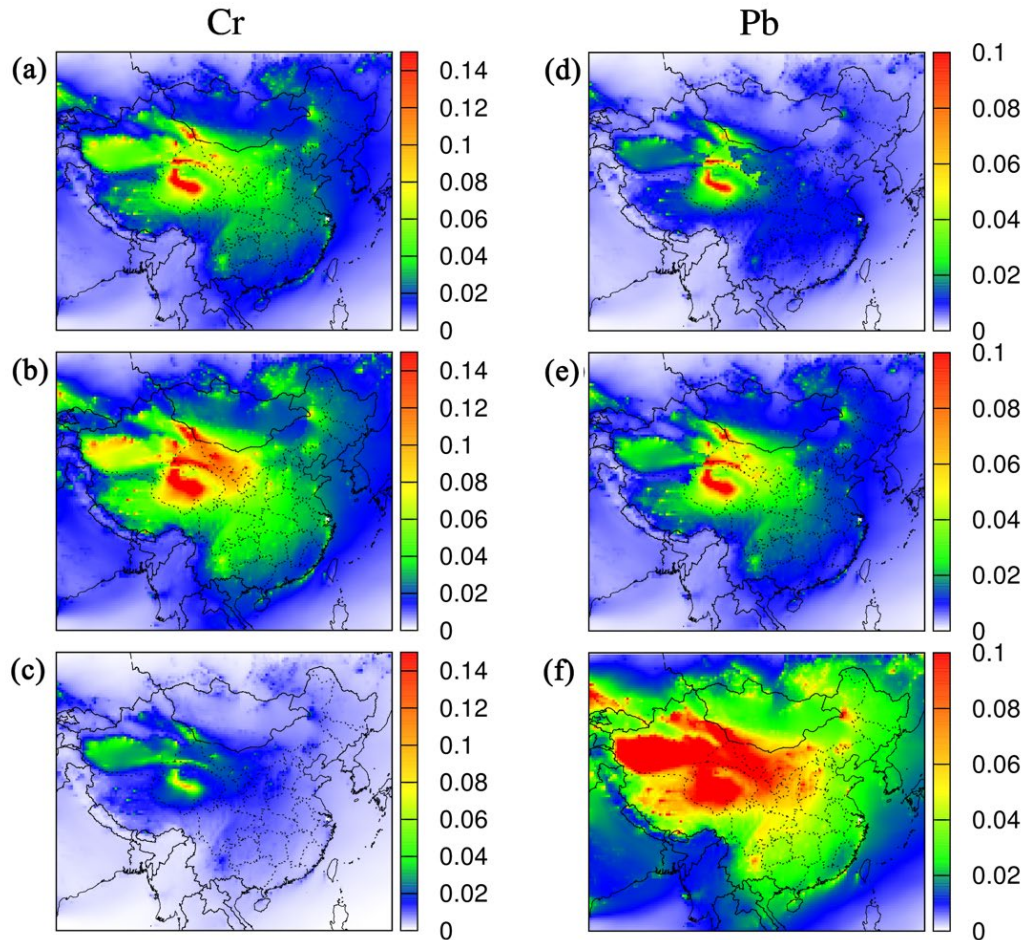
383 As discussed in the Introduction, many atmospheric studies assume that dust aerosol composition  
384 is similar to the composition of its parent soil. Here we also use the soil composition as an input  
385 dust profile in the model calculation to see how the modeled results are compared to that using the  
386 dust-PM<sub>2.5</sub> profile. For Cr, an obvious elevation of contribution was found by comparing the map  
387 using soil (a) and dust-PM<sub>2.5</sub> (b) profiles, with the hotspots of contribution ( $\sim 0.14 \mu\text{g}/\text{m}^3$ )  
388 distributed in northwest China. The region with dust aerosol contribution ranged from 0.02 to 0.08  
389  $\mu\text{g}/\text{m}^3$  covers most areas in China by using the dust-PM<sub>2.5</sub> profile. In contrast, the application of

390 the soil profile to the model reveals a significantly reduced area where the modeled Cr concentration  
391 from dust aerosols falls within the range of 0.02 to 0.08  $\mu\text{g}/\text{m}^3$ . For Pb, a significant difference is  
392 also found. The high contribution areas are also mainly distributed in northwest China for scenarios  
393 of applying soil and dust profiles, with the value up to 0.1  $\mu\text{g}/\text{m}^3$ . While the area with low dust  
394 aerosol contribution ( $<0.02 \mu\text{g}/\text{m}^3$ ) shrinks considerably in the scenario of applying soil profile.

395

396 The applied dust enrichment factors to modeled Cr in  $\text{PM}_{2.5}$  had an even stronger impact on modeled  
397 source apportionment (Fig. 3a-3b). The average dust source contribution to the total  $\text{PM}_{2.5}$  Cr  
398 concentration over China was calculated to be 0.03, and 0.05  $\mu\text{g}/\text{m}^3$  in the scenarios of applying  
399 soil and dust profiles, respectively. The model results for As, Cu, Mn, Ti and Zn (Fig. S11-S15) also  
400 show similar trends, indicating applying realistic enrichment factors to heavy metal concentrations  
401 in fine dust aerosols is critical to accurately model the sources of atmospheric heavy metals. These  
402 results demonstrate that it is not appropriate to assume dust aerosol composition is equal to soil  
403 composition, at least in air quality modeling.





404

405 **Figure 3.** Modeling of the contributions of dust aerosols to atmospheric Cr and Pb concentrations.

406 These results use the dust profiles of measured soil (a, d), dust-PM<sub>2.5</sub> (b, e), and the SPECIATE  
 407 datasets (c, f). The unit is  $\mu\text{g}/\text{m}^3$ .

408 [Figure 4](#) shows the Total Carcinogenic Risk (TCR) of the modeled atmospheric heavy metals (Cu,

409 Pb and Zn) for each province in Mainland, China. The modeled results using the dust-PM<sub>2.5</sub> and the

410 SPECIATE profiles are compared here. The carcinogenic risks lower than  $10^{-6}$  are considered

411 negligible, and risks above  $10^{-4}$  are not accepted by most international regulatory agencies ([Cheng](#)

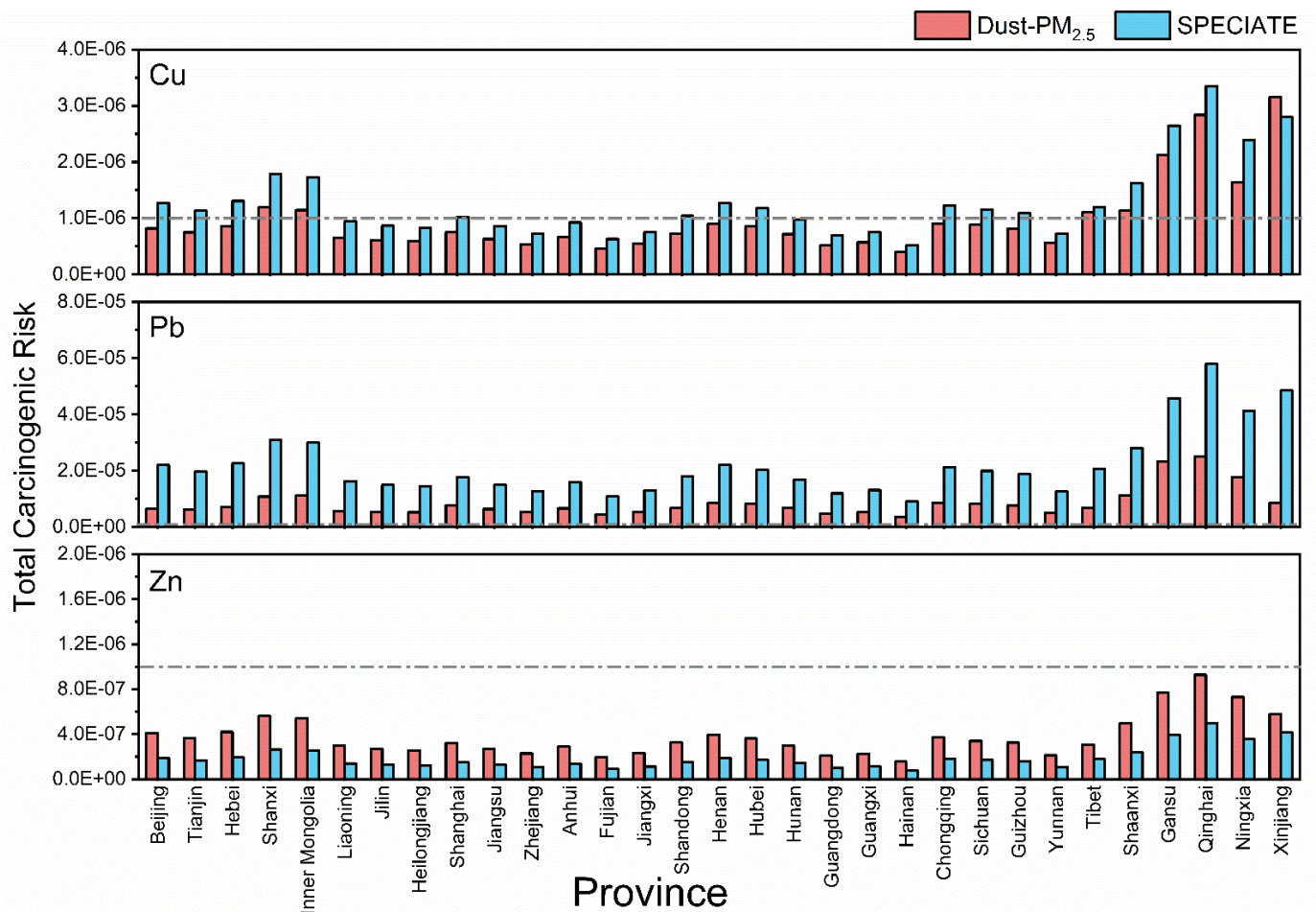
412 [et al., 2015](#); [Epa, 1989](#); [Luo et al., 2012](#)). For Cu, it is evident that using the SPECIATE profile

413 overestimated (the difference range up to  $\sim 7.5 \times 10^{-7}$ ) the TCR in China compared to using the dust-

414 PM<sub>2.5</sub> profile, as some regions exceed  $10^{-6}$ , the threshold value. For Pb, although all regions were

415 above  $10^{-6}$ , the TCR using the SPECIATE profile was greatly overestimated (the difference range is

416  $\sim 5.5 \times 10^{-6}$  -  $4.0 \times 10^{-5}$ ). The model results for Zn showed that all regions were not above  $10^{-6}$  but  
 417 significantly underestimated risks using the SPECIATE profile. This indicates that the health risk  
 418 assessment is also sensitive to dust composition profiles. Using the SPECIATE profile might be  
 419 problematic for assessing these risks.



420  
 421 **Figure 4.** Comparison of the total carcinogenic risk (TCR) of the modeled atmospheric heavy metals  
 422 for each province in Mainland, China between using the dust-PM<sub>2.5</sub> and SPECIATE profiles. Here,  
 423 the TCR of Cu, Pb and Zn were calculated. The grey dotted line is  $10^{-6}$ , the threshold value for  
 424 health concerns.  
 425

### 426 3.3 Field observation before, during and after a dust storm

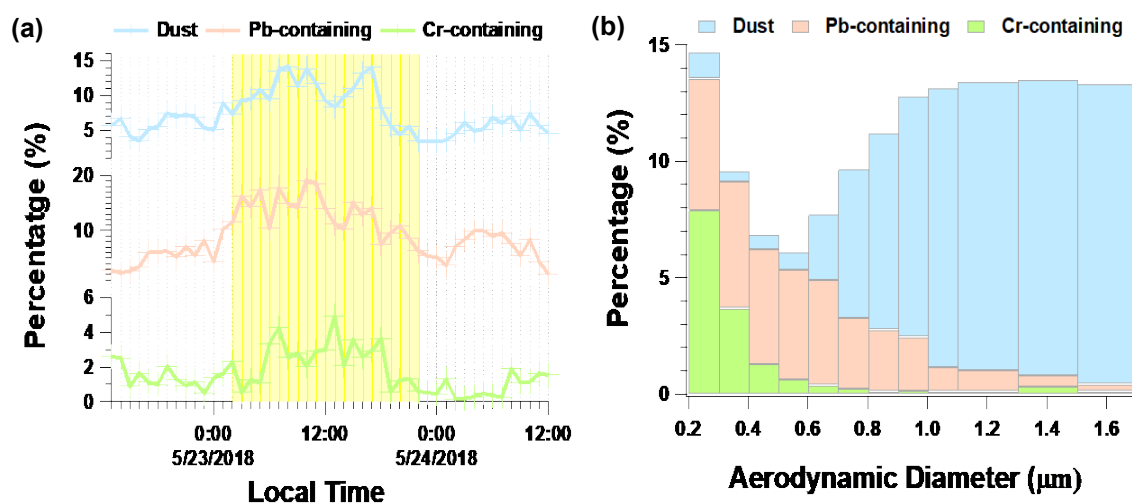
427 Our modeling results suggest that dust aerosol could be a major source of multiple heavy metals in  
428 PM<sub>2.5</sub> in China. Therefore, dust storms should significantly increase the concentrations of heavy  
429 metals in PM<sub>2.5</sub>. To test this idea, we studied a dust-storm plume, which originated from Mongolia  
430 and arrived in Shanghai (Huang et al., 2010) on 23 May 2018 (Fig. S16). Real-time single-particle  
431 mass spectra were generated by a single-particle mass spectrometer. Single particle mass  
432 spectrometry can offer detailed information on the chemically-resolved mixing state at the single-  
433 particle level. According to the similarities of the mass-to-charge ratio and peak intensity of  
434 characterized signals, “Dust” particles were classified via an adaptive resonance theory-based  
435 clustering method (ART-2a, see Method). The number fraction of *Dust* particles was ~4.94% before  
436 and after the dust storm and it increased to ~9.73% during the dust storm episode (Fig. 5a).

437  
438 *Dust* particle mass spectra also contained ion markers indicative of an array of heavy metals ( $m/z$   
439 55[Mn<sup>+</sup>], 51[V<sup>+</sup>], 207[Pb<sup>+</sup>], 63[Cu<sup>+</sup>], 75[As<sup>+</sup>], 91[AsO<sup>+</sup>], 52[Cr<sup>+</sup>], -84[CrO<sub>2</sub><sup>-</sup>], -100[CrO<sub>3</sub><sup>-</sup>]) (red  
440 sticks in Fig. S17), indicating the existence of heavy metals in the ambient dust aerosols. The time  
441 series of Pb-containing and Cr-containing particle number fractions showed similar trends to the  
442 *Dust* particles. When the dust storm arrived, both Pb-containing and Cr-containing particle fractions  
443 increased as the dust cluster fraction increased. Before and after the dust storm, the percentages of  
444 Pb-containing and Cr-containing particles that overlapped with the *Dust* cluster were 41% and 32%,  
445 respectively. However, this overlapped ratio increased to 86% and 71% during the dust storm  
446 episode. The increase of heavy metal particles in step with the dust particles indicated that the dust  
447 particles could be the dominant source of these heavy metal species during this dust storm episode.



448

449 We further analyzed the size-resolved number fraction of dust aerosol, Pb-containing, and Cr-  
450 containing particles during the dust storm episode (Fig. 5b). The number fraction of *Dust* particles  
451 increased with increasing aerodynamic diameter. For particles above 1.0  $\mu\text{m}$ , *Dust* accounted  
452 for >12% of the total particles during the storm. However, the Pb-containing and Cr-containing  
453 particles made up a larger number fraction of analyzed particles with decreasing particle diameter  
454 size (< 1  $\mu\text{m}$ ). The number fractions of Pb-containing and Cr-containing particles were 5.7% and  
455 7.9% of all mass spectra for particles from 0.2-0.3  $\mu\text{m}$ . This result was consistent with our laboratory  
456 results that there is high heavy metal enrichment in smaller dust particles and our modeling results  
457 that dust aerosol is likely a major source of atmospheric Pb and Cr over China.



458

459 **Figure 5.** Ambient dust aerosol measurements. (a) Temporal variation of the percentages of dust  
460 aerosol, Pb-containing, and Cr-containing particle clusters. The yellow shadow represents the dust  
461 storm episode. (b) Size-resolved number fraction of dust aerosol, Pb-containing, and Cr-containing  
462 particle clusters.

463

## 464 **4 Environmental implications**

465 In this study, many heavy metals were found to be highly enriched in fine (PM<sub>2.5</sub>) dust aerosols  
466 compared to their concentrations in the parent soils. We propose that heavy metals tend to be  
467 enriched in smaller soil aggregates (Ikegami et al., 2014). During the sandblasting process, the  
468 heavy metal enriched smaller soil aggregates are more likely to be ejected and form dust aerosols.  
469 This work finds that dust aerosols from different soils may have a range of heavy metal enrichment  
470 factors. To study the transfer of heavy metals from soils to the air, it is critical to have a complete  
471 set of enrichment factors for each major soil type. There exists a difference among the heavy metal  
472 enrichment factors from different soil samples. The variability in the EFs is likely due to differences  
473 in soil properties (soil texture and size distribution etc.) which may affect the sandblasting/saltation  
474 process. For example, the enrichment factors of heaviest metals for Soil S1, S10 and S11 were  
475 higher than other soils. The detailed reason is still unknown and needs further exploration. Moreover,  
476 air quality models, including CMAQ models and various CMB models, often use the dust chemical  
477 profiles from the US EPA's SPECIATE to calculate the contribution of fine dust aerosols to  
478 atmospheric heavy metals, which are outdated and could lead to significant errors in estimating the  
479 emission of heavy metals through dust generation. Without using proper dust profiles in estimating  
480 heavy metal emissions from dust generation, the contribution of fine dust aerosols to atmospheric  
481 heavy metals, and its associated health risks are likely significantly mistaken.

## 482 **5. Conclusions**

483 Dust generation and aerosolization are complex processes that may have certain chemical selectivity.

484 Here, we deployed a laboratory generator to produce dust aerosol with a realistic sandblasting  
485 process. The concentrations of heavy metals (including V, Cr, Mn, Co, Ni, Cu, Zn, As, Cd, Ba,  
486 Ti, and Pb) in soils and fine (PM<sub>2.5</sub>) and coarse (PM<sub>10</sub>) dust aerosols were measured. With  
487 research efforts to elucidate the enrichment process of heavy metal in dust aerosols comparing  
488 to their parent soils, our results fill the knowledge gaps of the compositional variation of heavy  
489 metal between the parent soils and the generated dust aerosols. Mn, Cd, Pb and other heavy  
490 metals were found to be highly enriched in fine (PM<sub>2.5</sub>) dust aerosols, which can be up to ~6.5-  
491 fold. These findings were also consistent with our field observation results. In addition, air  
492 quality models often use an outdated heavy metal profile for dust aerosols from the US EPA's  
493 SPECIATE database, which seems to be lack of enrichment between each particle size. We modeled  
494 the impact of the contribution of heavy metals in dust aerosol and their health risks in CMAQ,  
495 a widely used air quality model, and determined that atmospheric heavy metal concentrations  
496 over China, which drastically changed when we applied different dust profiles, such as the  
497 measured soil, dust-PM<sub>2.5</sub> profiles from this study, as well as the SPECIATE composition  
498 profiles. Our air quality modeling for China demonstrates that the calculated contribution of fine  
499 dust aerosols to atmospheric heavy metals, as well as their cancer risks, could have significant errors  
500 without using proper dust profiles.

## 501 **Supplement**

502 The supplement related to this article is available online at: <http://dx.doi.org/0.17632/byg6xk2fg9.1>.

503 **Data availability**

504 All data supporting this study and its findings will be available in an online data repository at:

505 <http://dx.doi.org/10.17632/wpphf8rd33.1>.

506 **Author contributions**

507 X.W. and J.C. conceptualized the work and designed the experiments. H.Z. and S.Z. led the air

508 quality modeling work. Q.G. lead the experimental work of heavy metal enrichment measurements.

509 J.Z. led the field observation. K.Z., Q.W., S.C., S.W., J.H., X.L. and H.C. helped in experimental

510 works. L.Z., L.W., Z.W., X.Y. and H.Z. helped in the experimental design and data analysis. Q.Y.

511 provided the data required for the air quality modeling. All authors contributed to the paper's writing.

512

513 **Competing interests**

514 The authors declare no competing interests.

515 **Disclaimer**

516 Publisher's note: Copernicus Publications remains neutral with regard to jurisdictional claims in

517 published maps and institutional affiliations.

518

## 519 **Acknowledgements**

520 The authors also thank Xingxing Wang and Xiangcheng Zeng for their help in heavy metal measurement.

## 521 **Financial support**

522 This work was partially supported by the National Natural Science Foundation of China (Nos.  
523 92044301, 42077193, 21906024). Comments from Dr. Camille Sultana greatly improved this  
524 manuscript.

## 525 **Reference**

526 Alfaro, S. C.: Influence of soil texture on the binding energies of fine mineral dust particles  
527 potentially released by wind erosion, *Geomorphology*, 93, 157-167,  
528 10.1016/j.geomorph.2007.02.012, 2008.

529 Alfaro, S. C., Gaudichet, A., Gomes, L., and Maille, M.: Modeling the size distribution of a  
530 soil aerosol produced by sandblasting, *Journal of Geophysical Research-Atmospheres*, 102, 11239-  
531 11249, 10.1029/97jd00403, 1997.

532 Ashrafi, K., Fallah, R., Hadei, M., Yarahmadi, M., and Shahsavani, A.: Source apportionment  
533 of total suspended particles (TSP) by positive matrix factorization (PMF) and chemical mass  
534 balance (CMB) modeling in Ahvaz, Iran, *Archives of environmental contamination and toxicology*,  
535 75, 278-294, 2018.

536 Balakrishna, G. and Pervez, S.: Source apportionment of atmospheric dust fallout in an urban-  
537 industrial environment in India, *Aerosol and Air Quality Research*, 9, 359-367, 2009.

538 Becagli, S., Caiazzo, L., Di Iorio, T., di Sarra, A., Meloni, D., Muscari, G., Pace, G., Severi,  
539 M., and Traversi, R.: New insights on metals in the Arctic aerosol in a climate changing world,  
540 *Science of The Total Environment*, 741, 140511, <https://doi.org/10.1016/j.scitotenv.2020.140511>,  
541 2020.

542 Brady, N. and Weil, R.: *The nature and properties of soils*, Pearson Education, Inc.0135133874,  
543 2008.

544 Bryant, R. G.: Recent advances in our understanding of dust source emission processes,  
545 *Progress in Physical Geography-Earth and Environment*, 37, 397-421, 10.1177/0309133313479391,  
546 2013.

547 Burezq, H.: Combating wind erosion through soil stabilization under simulated wind flow  
548 condition - Case of Kuwait, *International Soil and Water Conservation Research*, 8, 154-163,  
549 10.1016/j.iswcr.2020.03.001, 2020.

550 Chang, A. C., Warneke, J. E., Page, A. L., and Lund, L. J.: Accumulation of Heavy Metals in  
551 Sewage Sludge-Treated Soils, *Journal of Environmental Quality*, 13, 87-91,  
552 <https://doi.org/10.2134/jeq1984.00472425001300010016x>, 1984.

553 Cheng, I., Xu, X., and Zhang, L.: Overview of receptor-based source apportionment studies  
554 for speciated atmospheric mercury, *Atmospheric Chemistry and Physics*, 15, 7877-7895,  
555 10.5194/acp-15-7877-2015, 2015.

556 Ding, R. Q., Li, J. P., Wang, S. G., and Ren, F. M.: Decadal change of the spring dust storm in  
557 northwest China and the associated atmospheric circulation, *Geophysical Research Letters*, 32,  
558 10.1029/2004gl021561, 2005.

559 DoE, U.: The risk assessment information system (RAIS), Argonne, IL: US Department of  
560 Energy's Oak Ridge Operations Office (ORO), 2011.

561 EPA, A.: Risk assessment guidance for superfund. Volume I: human health evaluation manual  
562 (part a), EPA/540/1-89/002, 1989.

563 Evan, A. T., Flamant, C., Fiedler, S., and Doherty, O.: An analysis of aeolian dust in climate  
564 models, *Geophysical Research Letters*, 41, 5996-6001, 10.1002/2014gl060545, 2014.

565 Fu, Q., Zhuang, G., Li, J., Huang, K., Wang, Q., Zhang, R., Fu, J., Lu, T., Chen, M., Wang, Q.,  
566 Chen, Y., Xu, C., and Hou, B.: Source, long-range transport, and characteristics of a heavy dust  
567 pollution event in Shanghai, *Journal of Geophysical Research: Atmospheres*, 115,  
568 <https://doi.org/10.1029/2009JD013208>, 2010.

569 Fu, X., Wang, S. X., Cheng, Z., Xing, J., Zhao, B., Wang, J. D., and Hao, J. M.: Source,  
570 transport and impacts of a heavy dust event in the Yangtze River Delta, China, in 2011, *Atmospheric  
571 Chemistry and Physics*, 14, 1239-1254, 10.5194/acp-14-1239-2014, 2014.

572 Gholizadeh, A., Taghavi, M., Moslem, A., Neshat, A. A., Najafi, M. L., Alahabadi, A., Ahmadi,  
573 E., Asour, A. A., Rezaei, H., and Gholami, S.: Ecological and health risk assessment of exposure to  
574 atmospheric heavy metals, *Ecotoxicology and environmental safety*, 184, 109622, 2019a.

575 Gholizadeh, A., Taghavi, M., Moslem, A., Neshat, A. A., Lari Najafi, M., Alahabadi, A.,  
576 Ahmadi, E., Ebrahimi aval, H., Asour, A. A., Rezaei, H., Gholami, S., and Miri, M.: Ecological and  
577 health risk assessment of exposure to atmospheric heavy metals, *Ecotoxicology and Environmental  
578 Safety*, 184, 109622, <https://doi.org/10.1016/j.ecoenv.2019.109622>, 2019b.

579 Gillette, D. and Goodwin, P. A.: Microscale transport of sand-sized soil aggregates eroded by  
580 wind, *Journal of Geophysical Research*, 79, 4080-4084, 10.1029/JC079i027p04080, 1974.

581 Griggs, D. J. and Noguer, M.: Climate change 2001: the scientific basis. Contribution of  
582 working group I to the third assessment report of the intergovernmental panel on climate change,  
583 *Weather*, 57, 267-269, 2002.

584 Grini, A. and Zender, C. S.: Roles of saltation, sandblasting, and wind speed variability on  
585 mineral dust aerosol size distribution during the Puerto Rican Dust Experiment (PRIDE), *Journal  
586 of Geophysical Research-Atmospheres*, 109, 10.1029/2003jd004233, 2004.

587 Grini, A., Zender, C. S., and Colarco, P. R.: Saltation Sandblasting behavior during mineral  
588 dust aerosol production, *Geophysical Research Letters*, 29, 10.1029/2002gl015248, 2002.

589 Guenther, A. B., Jiang, X., Heald, C. L., Sakulyanontvittaya, T., Duhl, T., Emmons, L. K., and  
590 Wang, X.: The Model of Emissions of Gases and Aerosols from Nature version 2.1 (MEGAN2.1):  
591 an extended and updated framework for modeling biogenic emissions, *Geoscientific Model  
592 Development*, 5, 1471-1492, 10.5194/gmd-5-1471-2012, 2012.

593 Gunawardana, C., Goonetilleke, A., Egodawatta, P., Dawes, L., and Kokot, S.: Source

594 characterisation of road dust based on chemical and mineralogical composition, *Chemosphere*, 87,  
595 163-170, 10.1016/j.chemosphere.2011.12.012, 2012.

596 Ho, K. F., Lee, S. C., Chow, J. C., and Watson, J. G.: Characterization of PM<sub>10</sub> and PM<sub>2.5</sub>  
597 source profiles for fugitive dust in Hong Kong, *Atmospheric Environment*, 37, 1023-1032,  
598 10.1016/s1352-2310(02)01028-2, 2003.

599 Huang, K., Zhuang, G. S., Li, J. A., Wang, Q. Z., Sun, Y. L., Lin, Y. F., and Fu, J. S.: Mixing  
600 of Asian dust with pollution aerosol and the transformation of aerosol components during the dust  
601 storm over China in spring 2007, *Journal of Geophysical Research-Atmospheres*, 115,  
602 10.1029/2009jd013145, 2010.

603 Huebert, B. J., Bates, T., Russell, P. B., Shi, G. Y., Kim, Y. J., Kawamura, K., Carmichael, G.,  
604 and Nakajima, T.: An overview of ACE-Asia: Strategies for quantifying the relationships between  
605 Asian aerosols and their climatic impacts, *Journal of Geophysical Research-Atmospheres*, 108,  
606 10.1029/2003jd003550, 2003.

607 Huneus, N., Schulz, M., Balkanski, Y., Griesfeller, J., Prospero, J., Kinne, S., Bauer, S.,  
608 Boucher, O., Chin, M., Dentener, F., Diehl, T., Easter, R., Fillmore, D., Ghan, S., Ginoux, P., Grini,  
609 A., Horowitz, L., Koch, D., Krol, M. C., Landing, W., Liu, X., Mahowald, N., Miller, R., Morcrette,  
610 J. J., Myhre, G., Penner, J., Perlwitz, J., Stier, P., Takemura, T., and Zender, C. S.: Global dust model  
611 intercomparison in AeroCom phase I, *Atmospheric Chemistry and Physics*, 11, 7781-7816,  
612 10.5194/acp-11-7781-2011, 2011.

613 Ikegami, M., Yoneda, M., Tsuji, T., Bannai, O., and Morisawa, S.: Effect of Particle Size on  
614 Risk Assessment of Direct Soil Ingestion and Metals Adhered to Children's Hands at Playgrounds,  
615 *Risk Analysis*, 34, 1677-1687, 10.1111/risa.12215, 2014.

616 Kaufman, Y. J., Tanre, D., and Boucher, O.: A satellite view of aerosols in the climate system,  
617 *Nature*, 419, 215-223, 10.1038/nature01091, 2002.

618 Kettler, T. A., Doran, J. W., and Gilbert, T. L.: Simplified Method for Soil Particle-Size  
619 Determination to Accompany Soil-Quality Analyses, *Soil Science Society of America Journal*, 65,  
620 849-852, <https://doi.org/10.2136/sssaj2001.653849x>, 2001.

621 Kok, J. F., Ward, D. S., Mahowald, N. M., and Evan, A. T.: Global and regional importance of  
622 the direct dust-climate feedback, *Nature Communications*, 9, 10.1038/s41467-017-02620-y, 2018.

623 Kok, J. F., Storelvmo, T., Karydis, V. A., Adebisi, A. A., Mahowald, N. M., Evan, A. T., He,  
624 C., and Leung, D. M.: Mineral dust aerosol impacts on global climate and climate change, *Nature*  
625 *Reviews Earth & Environment*, 10.1038/s43017-022-00379-5, 2023.

626 Lafon, S., Alfaro, S. C., Chevaillier, S., and Rajot, J. L.: A new generator for mineral dust  
627 aerosol production from soil samples in the laboratory: GAMEL, *Aeolian Research*, 15, 319-334,  
628 <https://doi.org/10.1016/j.aeolia.2014.04.004>, 2014.

629 Lafon, S., Sokolik, I. N., Rajot, J. L., Caquineau, S., and Gaudichet, A.: Characterization of  
630 iron oxides in mineral dust aerosols: Implications for light absorption, *Journal of Geophysical*  
631 *Research-Atmospheres*, 111, 10.1029/2005jd007016, 2006.

632 Li, L., Huang, Z. X., Dong, J. G., Li, M., Gao, W., Nian, H. Q., Fu, Z., Zhang, G. H., Bi, X. H.,  
633 Cheng, P., and Zhou, Z.: Real time bipolar time-of-flight mass spectrometer for analyzing single  
634 aerosol particles, *International Journal of Mass Spectrometry*, 303, 118-124,  
635 10.1016/j.ijms.2011.01.017, 2011.

636 Liu, Q., Liu, X., Liu, T., Kang, Y., Chen, Y., Li, J., and Zhang, H.: Seasonal variation in particle  
637 contribution and aerosol types in Shanghai based on satellite data from MODIS and CALIOP,

638 Particuology, 51, 18-25, <https://doi.org/10.1016/j.partic.2019.10.001>, 2020.

639 Liu, Q., Wang, Y., Kuang, Z., Fang, S., Chen, Y., Kang, Y., Zhang, H., Wang, D., and Fu, Y.:  
640 Vertical distributions of aerosol optical properties during haze and floating dust weather in Shanghai,  
641 Journal of Meteorological Research, 30, 598-613, 10.1007/s13351-016-5092-4, 2016.

642 Liu, X. D., Yin, Z. Y., Zhang, X. Y., and Yang, X. C.: Analyses of the spring dust storm  
643 frequency of northern China in relation to antecedent and concurrent wind, precipitation, vegetation,  
644 and soil moisture conditions, Journal of Geophysical Research-Atmospheres, 109,  
645 10.1029/2004jd004615, 2004.

646 Lowenthal, D. H., Watson, J. G., Koracin, D., Chen, L.-W. A., Dubois, D., Vellore, R., Kumar,  
647 N., Knipping, E. M., Wheeler, N., and Craig, K.: Evaluation of regional-scale receptor modeling,  
648 Journal of the Air & Waste Management Association, 60, 26-42, 2010.

649 Luo, X.-S., Ding, J., Xu, B., Wang, Y.-J., Li, H.-B., and Yu, S.: Incorporating bioaccessibility  
650 into human health risk assessments of heavy metals in urban park soils, Science of the Total  
651 Environment, 424, 88-96, 2012.

652 Lv, M., Hu, A., Chen, J., and Wan, B.: Evolution, Transport Characteristics, and Potential  
653 Source Regions of PM<sub>2.5</sub> and O<sub>3</sub> Pollution in a Coastal City of China during 2015–2020,  
654 Atmosphere, 12, 1282, 2021.

655 Middleton, N., Tozer, P., and Tozer, B.: Sand and dust storms: underrated natural hazards,  
656 Disasters, 43, 390-409, 10.1111/disa.12320, 2019.

657 Miller, M. S., Friedlander, S. K., and Hidy, G. M.: A chemical element balance for the Pasadena  
658 aerosol, Journal of Colloid and Interface Science, 39, 165-176, [https://doi.org/10.1016/0021-](https://doi.org/10.1016/0021-9797(72)90152-X)  
659 9797(72)90152-X, 1972.

660 Moya, J., Phillips, L., Schuda, L., Wood, P., Diaz, A., Lee, R., Clickner, R., Birch, R., Adjei,  
661 N., and Blood, P.: Exposure factors handbook: 2011 edition, US Environmental Protection Agency,  
662 2011.

663 Naderizadeh, Z., Khademi, H., and Ayoubi, S.: Biomonitoring of atmospheric heavy metals  
664 pollution using dust deposited on date palm leaves in southwestern Iran, *Atmósfera*, 29, 141-155,  
665 10.20937/ATM.2016.29.02.04, 2016.

666 Parajuli, S. P., Zobeck, T. M., Kocurek, G., Yang, Z. L., and Stenchikov, G. L.: New insights  
667 into the wind-dust relationship in sandblasting and direct aerodynamic entrainment from wind  
668 tunnel experiments, Journal of Geophysical Research-Atmospheres, 121, 1776-1792,  
669 10.1002/2015jd024424, 2016.

670 Perlwitz, J. P., Pérez García-Pando, C., and Miller, R. L.: Predicting the mineral composition  
671 of dust aerosols – Part 1: Representing key processes, *Atmos. Chem. Phys.*, 15, 11593-11627,  
672 10.5194/acp-15-11593-2015, 2015.

673 Pongkiatkul, P. and Kim Oanh, N. T.: Assessment of potential long-range transport of  
674 particulate air pollution using trajectory modeling and monitoring data, *Atmospheric Research*, 85,  
675 3-17, <https://doi.org/10.1016/j.atmosres.2006.10.003>, 2007.

676 Prospero, J. M., Ginoux, P., Torres, O., Nicholson, S. E., and Gill, T. E.: Environmental  
677 characterization of global sources of atmospheric soil dust identified with the Nimbus 7 Total Ozone  
678 Mapping Spectrometer (TOMS) absorbing aerosol product, *Reviews of geophysics*, 40, 2-1-2-31,  
679 2002.

680 Samiksha, S., Raman, R. S., Nirmalkar, J., Kumar, S., and Sirvaiya, R.: PM<sub>10</sub> and PM<sub>2.5</sub>  
681 chemical source profiles with optical attenuation and health risk indicators of paved and unpaved



682 road dust in Bhopal, India, *Environmental Pollution*, 222, 477-485, 2017.

683 Santos, J. M., Reis, N. C., Galvão, E. S., Silveira, A., Goulart, E. V., and Lima, A. T.: Source  
684 apportionment of settleable particles in an impacted urban and industrialized region in Brazil,  
685 *Environmental Science and Pollution Research*, 24, 22026-22039, 2017.

686 Shangguan, Y., Zhuang, X., Querol, X., Li, B., Moreno, N., Trechera, P., Sola, P. C., Uzu, G.,  
687 and Li, J.: Characterization of deposited dust and its respirable fractions in underground coal mines:  
688 Implications for oxidative potential-driving species and source apportionment, *International Journal*  
689 *of Coal Geology*, 258, 104017, <https://doi.org/10.1016/j.coal.2022.104017>, 2022.

690 Shao, Y. and Dong, C. H.: A review on East Asian dust storm climate, modelling and  
691 monitoring, *Global and Planetary Change*, 52, 1-22, 10.1016/j.gloplacha.2006.02.011, 2006.

692 Shao, Y. and Raupach, M. R.: Effect of saltation bombardment on the environment of dust by  
693 wind, *Journal of Geophysical Research-Atmospheres*, 98, 12719-12726, 10.1029/93jd00396, 1993.

694 Shao, Y. P., Klose, M., and Wyrwoll, K. H.: Recent global dust trend and connections to climate  
695 forcing, *Journal of Geophysical Research-Atmospheres*, 118, 11107-11118, 10.1002/jgrd.50836,  
696 2013.

697 Shao, Y. P., Raupach, M. R., and Leys, J. F.: A model for predicting aeolian sand drift and dust  
698 entrainment on scales from paddock to region, *Australian Journal of Soil Research*, 34, 309-342,  
699 10.1071/sr9960309, 1996.

700 Shi, J., Li, Z., Sun, Z., Han, X., Shi, Z., Xiang, F., and Ning, P.: Specific features of heavy  
701 metal pollutant residue in PM<sub>2.5</sub> and analysis of their damage level for human health in the urban  
702 air of Kunming, *J. Saf. Environ*, 18, 795-800, 2018.

703 Simon, H., Beck, L., Bhave, P. V., Divita, F., Hsu, Y., Luecken, D., Mobley, J. D., Pouliot, G.  
704 A., Reff, A., and Sarwar, G.: The development and uses of EPA's SPECIATE database, *Atmospheric*  
705 *Pollution Research*, 1, 196-206, 2010.

706 Sullivan, R., Guazzotti, S., Sodeman, D., and Prather, K.: Direct observations of the  
707 atmospheric processing of Asian mineral dust, *Atmospheric Chemistry and Physics*, 7, 1213-1236,  
708 2007.

709 Sun, R., Wang, H., Ma, X., Chen, Y., Zhao, B., Qin, Y., Zhang, H., and Ye, W.: Aerosol optical  
710 properties and formation mechanism of a typical air pollution episode in Shanghai during different  
711 weather condition periods, *Acta Scientiae Circumstantiae*, 37, 814-823, 2017.

712 Tang, M. J., Cziczo, D. J., and Grassian, V. H.: Interactions of Water with Mineral Dust Aerosol:  
713 Water Adsorption, Hygroscopicity, Cloud Condensation, and Ice Nucleation, *Chemical Reviews*,  
714 116, 4205-4259, 10.1021/acs.chemrev.5b00529, 2016.

715 Textor, C., Schulz, M., Guibert, S., Kinne, S., Balkanski, Y., Bauer, S., Berntsen, T., Berglen,  
716 T., Boucher, O., Chin, M., Dentener, F., Diehl, T., Easter, R., Feichter, H., Fillmore, D., Ghan, S.,  
717 Ginoux, P., Gong, S., Kristjansson, J. E., Krol, M., Lauer, A., Lamarque, J. F., Liu, X., Montanaro,  
718 V., Myhre, G., Penner, J., Pitari, G., Reddy, S., Seland, O., Stier, P., Takemura, T., and Tie, X.:  
719 Analysis and quantification of the diversities of aerosol life cycles within AeroCom, *Atmospheric*  
720 *Chemistry and Physics*, 6, 1777-1813, 10.5194/acp-6-1777-2006, 2006.

721 Urrutia-Pereira, M., Rizzo, L. V., Staffeld, P. L., Chong-Neto, H. J., Viegi, G., and Sole, D.:  
722 Dust from the Sahara to the American Continent: Health impacts, *Allergologia Et*  
723 *Immunopathologia*, 49, 187-194, 10.15586/aei.v49i4.436, 2021.

724 Wang, L., Li, H., Zhang, W., Qi, J., Tian, H., Huang, K., Chen, D., and Guo, J.: Regional  
725 Pollution Characteristics of Heavy Metals in PM<sub>2.5</sub>, *Research of Environmental Sciences*, 34, 849-

726 862, 2021.

727 Wu, F., Cheng, Y., Hu, T., Song, N., Zhang, F., Shi, Z., Hang Ho, S. S., Cao, J., and Zhang, D.:  
728 Saltation–Sandblasting Processes Driving Enrichment of Water-Soluble Salts in Mineral Dust,  
729 Environmental Science & Technology Letters, 2022.

730 Xia, Z., Fan, X., Huang, Z., Liu, Y., Yin, X., Ye, X., and Zheng, J.: Comparison of Domestic  
731 and Foreign PM<sub>2.5</sub> Source Profiles and Influence on Air Quality Simulation, Research of  
732 Environmental Sciences, 30, 359-367, 2017.

733 Yang, Y. Q., Hou, Q., Zhou, C. H., Liu, H. L., Wang, Y. Q., and Niu, T.: Sand/dust storm  
734 processes in Northeast Asia and associated large-scale circulations, Atmospheric Chemistry and  
735 Physics, 8, 25-33, 10.5194/acp-8-25-2008, 2008.

736 Ying, Q., Feng, M., Song, D., Wu, L., Hu, J., Zhang, H., Kleeman, M. J., and Li, X.: Improve  
737 regional distribution and source apportionment of PM<sub>2.5</sub> trace elements in China using inventory-  
738 observation constrained emission factors, Science of the total environment, 624, 355-365, 2018.

739 Zhang, H. R. and Tripathi, N. K.: Geospatial hot spot analysis of lung cancer patients correlated  
740 to fine particulate matter (PM<sub>2.5</sub>) and industrial wind in Eastern Thailand, Journal of Cleaner  
741 Production, 170, 407-424, 10.1016/j.jclepro.2017.09.185, 2018.

742 Zhuang, G. S., Guo, J. H., Yuan, H., and Zhao, C. Y.: The compositions, sources, and size  
743 distribution of the dust storm from China in spring of 2000 and its impact on the global environment,  
744 Chinese Science Bulletin, 46, 895-901, 10.1007/bf02900460, 2001.

745

746